

Artificial Intelligence in Mechanical Manufacturing: From Machine Learning to Generative Pre-trained Transformer

Xu Zheng, Jemal H. Abawajy, Haruna Chiroma and Shafi'i Muhammad Abdulhamid
(Guest editors)

ORIGINAL ARTICLE

OPEN ACCESS

The state diagnosis method of metal enclosed gas insulation complete equipment based on deep learning algorithms

Jiayi Wang^{1,*}, Dianbo Zhou¹, Yuan Fang², Zhenze Long¹, Yuhang He¹, Xinyu Luo¹, and Yang Zou³

¹ Electric Power Research Institute, State Grid Sichuan Electric Power Company, Chengdu 610048, Sichuan, PR China

² State Grid Sichuan Electric Power Company, Chengdu 610042, Sichuan, PR China

³ State Grid Jiangxi Electric Power Company, Nanchang 330001, Jiangxi, PR China

Received: 9 September 2025 / Accepted: 5 January 2026

Abstract. The reliable operation of metal-enclosed gas-insulated equipment is crucial to high-voltage power systems, and accurate diagnosis of its status is the key to ensuring safe and efficient operation of the power grid. Accurate state diagnostics help to prevent gas-insulated equipment failures, ensuring stable and efficient operation of the electricity grid. The existing methods are difficult to effectively capture the temporal and sequential characteristics of partial discharge (PD) signals, resulting in insufficient recognition accuracy for complex defects such as conductor protrusions (C-type), surface contamination (S-type), and floating electrodes (F-type). At the same time, the on-site environmental noise interference is large, and the fault samples, especially the severe defect samples, are rare and unbalanced. In addition, the gas state is easily affected by temperature and pressure, which makes the existing diagnostic models weak in generalization ability and poor in real-time performance, making it difficult to meet the urgent needs of high-voltage power grids for accurate, online, and efficient diagnosis of equipment status. This limitation restricts timely and precise fault detection, leads to equipment failure, and operational disruptions pave the way for deep learning algorithms. Thus, the research proposes a Long Short-Term Memory based Gas Insulation State Diagnostics (LSTM-GISD) method for accurate fault detection and state diagnostics in gas insulation equipment. The study utilizes sensor data from critical vital components, including gas pressure, temperature, partial discharge, and electrical parameters, to accurately assess the operational state of gas insulated as a dielectric medium in high-voltage equipment. The methodology includes data preprocessing feature extraction to identify the relevant characteristics of PD signals. The LSTM-based Recurrent Neural Network (RNN) algorithm is used for model training to improve the classification of PD patterns and diagnose the operational state of gas insulation switch gear equipment, enhancing fault detection accuracy and supporting maintenance strategies. The model's effectiveness is evaluated using various metrics, including accuracy, precision, and recall. It focuses on their ability to identify both normal and fault states (C, S, F types) of equipment with improved reliability. The study results demonstrate improved fault detection speed in terms of computational time, accuracy and robustness in detecting faults and predicting potential failure states in equipment maintenance practices.

Keywords: Gas insulated switchgear / state diagnostics / long short-term memory / recurrent neural network / high-voltage power grids / partial discharge

1 Introduction

In modern electrical power systems, metal-enclosed Gas Insulation Switchgear (GIS) complete equipment is important because of its compactness, reliability, and low maintenance requirements. Despite its advantages, GIS is prone to different types of faults and degradations

over time, jeopardizing the efficiency and safety of the distributed power networks [1]. The metal enclosed gas is usually sulfur hexafluoride (SF₆). As a complete set of distribution equipment that seals high-voltage electrical components in a metal shell filled with insulating gas, metal enclosed gas insulated switchgear utilizes the excellent insulation and arc extinguishing performance of SF₆ gas to achieve high-voltage level power transmission and control in a compact space. It has the advantages of small

* e-mail: jiayi_wang2012@163.com

footprint, high reliability, and low environmental impact, and is widely used in urban substations and high-voltage transmission systems. The insulating system of the high-voltage equipment that makes up the electric power system must be in a condition that ensures correct operation for the equipment to function dependably [2]. Making decisions about high-voltage equipment maintenance, replacement, or repair to prevent expensive unplanned shutdowns caused by premature insulation failure is still a difficult task that necessitates a thorough evaluation of the electrical insulation of various in-service components. The cost of the in-service actions for utilities may be much greater, depending on the machinery and kind of insulation system employed in its design configuration [3]. PD activity measurement is one of the metrics considered in power transformer preventative maintenance. A PD is an electrical discharge that partially spans the dielectric medium between two conduction portions. It is a pre-breakdown occurrence. PD may or may not happen next to a conductor when high-voltage stress is present [4]. PD pattern properties, such as PD charge and inception voltage, are crucial as evaluation criteria in diagnostic systems employing PD classifiers for high-voltage electrical insulation [5]. Energy is released in conjunction with partial discharge in the form of ozone and nitrogen oxide emissions, acoustic emissions in the form of sound at ultrasonic ranges, and electromagnetic emissions in heat, light, and radio waves. Despite the tiny partial discharge magnitudes (approximately 5–10 eV), they drastically reduce the breakdown voltage and onset corona, which eventually causes the insulation in the GIS to deteriorate and ultimately collapse [6] gradually. Corona discharge is a type of partial discharge, usually referring to discharge outside the equipment. However, in GIS internal discharge monitoring, partial discharge is a more accurate term [7]. A stable PD starts when the GIS is powered at the standard operational voltage. Due to SF₆ gas degradation, a total breakdown of the GIS may finally happen after a specific amount of continuous PD or when the GIS is experiencing an overvoltage. As a result of the PD action, the equipment's withstand voltage significantly drops [8]. The dielectric performance and thermal conductivity of SF₆ are the most important characteristics when it comes to GIS, as they help determine the size of the gap that must be left between the inside of the tube or central conductor and the equipment's current rating. SF₆ is perfect for this application because of its strong dielectric strength and thermal conductivity. Transmission system substations use this equipment to hold vast amounts of SF₆. However, leakage rates are closely watched [9].

The advancement of deep learning (DL) algorithms offers unprecedented capacities in the recognition of patterns, detection of anomalies and predictive maintenance. It is possible to improve the efficacy and accuracy of fault diagnosis by utilizing advanced computational techniques in GIS equipment [10]. By processing enormous sensor information, the DL algorithms can identify very small patterns and point out the possible problems and issues in real-time solutions to avert the most difficult errors [11]. Sensors are usually placed at different locations in power plants to measure sensor data continually. Data

processing and feature extraction are done to find any irregularities or damage to the structures and systems. Plant outages can result in less revenue loss since non-destructive testing (NDT) can be carried out utilizing continually obtained sensor data without stopping plant activities [12]. LSTM, as an improved model of recurrent neural networks (RNNs), effectively solves the problems of gradient vanishing and long-term dependency forgetting that traditional RNNs are prone to when dealing with long sequences by introducing gating mechanisms. The core structure of its forget gate, input gate, and output gate can selectively remember or forget historical information, making it particularly suitable for analyzing nonlinear signals with temporal correlations [13–15]. Given that partial discharge (PD) patterns are essentially time-series data that vary periodically with voltage phase, LSTM can deeply explore the dynamic characteristics of their phase distribution and amplitude evolution, providing a powerful modeling tool for accurate diagnosis of GIS equipment states. Therefore, this paper chooses LSTM to construct a GIS state diagnosis model. The Long Short-Term Memory network model was developed as an improvement of Recurrent Neural Networks owing to the shortcomings of traditional RNNs with gradient vanishing and forgetting long-term dependencies, when dealing with long sequences. Unlike standard RNNs, the LSTM model utilizes gate structures to determine whether to keep or forget the previous time steps. Each time step can decide and filter attendance of historical information which gives LSTM a solid rationale for time-series analysis. Since the Partial Discharge signals are temporally relevant and have a strong correlation to the phase of the voltage cycles, the LSTM model is applied to capture these PD pattern evolutionary characteristics, providing a basis for diagnosing the operational condition of metals enclosed gas-insulated equipment. Numerous methods have been used to carry out automated PD fault recognition, including deep learning (DL) and machine learning (ML) [16].

1.1 Problem statement and research novelty

Precise state diagnostic of metal-enclosed gas-insulation apparatus is essential for the dependability and security of high-voltage power systems. Timely and accurate problem detection is hampered by traditional diagnostic tools' inability to analyze the temporal and sequential character of partial discharge (PD) patterns. A new technique called Long Short-Term Memory Gas Insulation State Diagnostics (LSTM-GISD) is presented in this study. It improves defect detection accuracy by using sensor data, including temperature, pressure, and PD signals, as well as deep learning techniques. This method improves the classification of PD patterns, providing a reliable and effective way to identify problems with gas insulation equipment and anticipate future breakdowns. The main innovation of this article lies in: 1) utilizing the gate structure of LSTM to dynamically learn and remember the evolution law of partial discharge (PD) patterns in time series, effectively capturing the temporal dependence and long-term correlation characteristics of PD signals that are difficult to handle by traditional methods; 2) By integrating

multi-source sensor data, a more comprehensive state assessment model has been constructed, which improves the accuracy and robustness of diagnosis; 3) Specially enhanced the ability to identify rare and dangerous F-type faults, and supported predictive maintenance by quantifying the severity, providing efficient and reliable ideas for the intelligent operation and maintenance of GIS equipment. Compared to CNN-GRU and CNN-BiLSTM, which rely on a CNN to extract spatial features and then process time series using a recurrent network, this is essentially a two-stage spatial-temporal analysis. This paper's LSTM-GISD directly models time series features extracted from PD signals, focusing on capturing the dynamic evolution and long-term dependencies of PD patterns within the voltage phase cycle. This approach better reflects the nature of PD time series data. The Long Short-Term Memory based diagnosis method selectively memorizes key historical information through a gating mechanism. Its relatively simple structure avoids the high computational overhead associated with CNNs. While maintaining a high recognition rate for rare faults like Type F, it achieves superior computational efficiency, making it more suitable for real-time online diagnosis applications.

1.2 Main contributions

The paper presents a state diagnosis method based on Long Short-Term Memory for gas-insulated switchgear, which uses deep learning to improve the precision of fault diagnosis in gas-insulated equipment.

The system uses sensor data, such as partial discharge signals and gas pressure, to precisely evaluate and diagnose the condition of metal-enclosed gas-insulated switchgear.

By increasing fault detection robustness and accuracy, the proposed Long Short-Term Memory based diagnosis method promotes better maintenance practices and operational dependability.

1.3 Organization of the paper

The paper's structure is as follows: [Section 2](#) discusses various fault detection methods in GIS using multiple ML techniques. [Section 3](#) examines the proposed analysis of various PD methods and classification based on deep learning methods. [Section 4](#) employs the results and discussions, experimental setup, and graphical representation of the result metrics. Finally, the paper concludes in [Section 5](#), discussing the limitations and future works.

2 Related works

Jin et al. [17] suggested a residual BP neural network-based enhanced transformer failure diagnostic technique. By stacking several residual network modules, this technique deepens the BP neural network and combines and expands gas feature data through an enhanced BP neural network. SVM is added to the improved residual BP neural network to evaluate the recovered feature vectors at each layer, accurately filter out feature vectors, and raise their

weights. Extracting gas feature information with more important feature differences after fusion expansion effectively improves diagnostic accuracy using multi-layer neural network mapping. Its drawbacks are high computational complexity, sluggish convergence rate, and vulnerability to local optima.

Tuyet-Doan et al. [18] presented a Shared Knowledge-based Contrastive Federated Learning (SK-CFL) for Intelligent Electronic Devices (IEDs) to diagnose Parkinson's disease (PD) in various noisy situations. By merging contrastive learning with federated learning principles, the proposed SK-CFL enables IEDs to acquire and exchange knowledge about noise patterns and PD jointly. While maintaining data privacy, the suggested system can identify representations between the same patterns across several IEDs. Results from experiments with PD diagnosis in GIS demonstrate that the suggested SK-CFL improves fault diagnosis performance, especially in novel and unfamiliar situations. Limitations include validating the proposed approach, PRPD tests with different gas pressures and further measurements for fault data.

Karandaev et al. [19] aimed to develop an expert system whose main method is the mathematical processing of partial discharge (PD) trends to identify insulation breaches, track their growth, and assess the system's risk. The goal is to find the transformer's state and classify it into one of the three widely accepted categories—Normal, Poor, or Critical—. This paper's contribution is the first validation of a single generalized metric based on online PD parameter monitoring characterizing transformer insulation status. Mathematical processing makes use of fuzzy logic methods. The insulation state indicator is the sole deterministic parameter that would be used to generalize the set of diagnostic variables. Creating and implementing intelligent online state monitoring systems for the metals industry is a pertinent IIoT-based upgrade area.

Li et al. [20] presented a GIS operational state prediction approach based on the convolutional neural network (CNN) and gated recurrent unit (GRU) mixed neural network. To evaluate their status, defects, past test results, and online monitoring data, they are combined with AHP and multi-level variable weight evaluation ideas. Equipment status correlation analysis and status prediction models are then built, and characteristic parameters are explored through the organic combination of quantitative and qualitative indicators. Correspondence between the states of the GIS. The approach's viability and correctness are confirmed through example analysis; compared to the GRU and long short-term memory (LSTM) models, it performs more efficiently and accurately in predictions.

Alsumaidae et al. [21] thoroughly analyzed three approaches: 1D-CNN, LSTM, and 1D-CNN-LSTM hybrid models to determine the most suitable deep learning strategy for detecting corona defects. The best model is the hybrid 1D-CNN-LSTM model, which has great accuracy in frequency and time domains. To find defects, this model examines the sound waves produced by switchgear. The study examines how well the model performs in frequency

and time domains. The suggested technique worked well and might be improved for real-time simulations, especially those involving the industrial sector.

Bampoula et al. [22] proposed a transformer encoder and LSTM-Autoencoder combination as a predictive maintenance method to allow asset failure predictions through temporal and geographic data series. A software prototype incorporates these neural networks. An industry case study on metal processing provided the dataset utilized to train and evaluate the models. The ultimate objective is to train an estimating model for remaining usable life (RUL). One drawback of the suggested method is that it requires numerous neural networks to determine the machine's status when working with higher-resolution data with many labels.

A technique based on enhanced deep learning for identifying partial discharge faults in GIS equipment was suggested by Hu et al. [23]. Initially, the GIS equipment's audio data is filtered using a Simple Power Normalized Cepstral Coefficient (SPNCC). The attention mechanism is intended to extract deeper data features. Secondly, a convolutional neural network obtains the spatial correlation between audio data streams. A bi-directional long short-term memory (BiLSTM) network is used to predict the next time slice data stream and get the temporal correlation of audio. Ultimately, the accuracy of GIS equipment's partial discharge identification technique is increased by establishing the partial discharge fault identification model based on enhanced SPNCC-CNN BiLSTM-multi-att. The intricate mapping link between features and states will be solved in the following stage of the primary endeavor.

A GIS PD fault diagnosis method based on an improved whale optimization algorithm (IWOA) was proposed by Sun et al. [24] to diagnose the PD in gas-insulated switchgear (GIS) more effectively. IWOA optimizes variational mode decomposition (VMD) and support vector machine (SVM) to enhance performance by adaptively determining the appropriate parameters. A laboratory GIS PD platform collects four types of PD fault signals (point discharge, particle discharge, floating discharge, and air-gap discharge). In addition, 33 feature vectors' dimensions are reduced to 7 by using the principal component analysis (PCA) approach to reduce the initial feature vectors' dimensions. At last, SVM based on IWOA is used to train and test the experimental data to diagnose GIS PD and detect various PD fault kinds. The accuracy of the fault diagnosis techniques above is higher. Nevertheless, many issues persist, including the wavelet basis function's limitations, high computational complexity, and lengthy computation times.

Cong et al. [25] first setup, a 220 kV GIS provides an experimental platform for partial discharge and four common defect models—insulator fouling, insulator air gap, floating electrode, and metal protrusions. The UHF approach and the pulse current method are used to gather the partial discharge signals of different types of faults. The suggested diagnosis technique of the BP neural network and improved DS evidence theory incorporate the fusion decision of PD signal based on time-resolved partial discharge and phase-resolved partial discharge. The proposed diagnosis

method identifies faults by introducing the degree of evidence fusion. The findings demonstrate the ability of the suggested recognition method to reject incorrect diagnoses and thoroughly provide helpful information.

This trend of deep learning-enabled defect diagnosis extends beyond power systems, as seen in structural health monitoring and manufacturing quality control [26,27]. However, current research in diagnosing the condition of metal-enclosed gas-insulated devices indicates a few main limitations. Conventional machine-learning models for partial discharge (PD) signals (e.g., BP neural networks and Support Vector Machines) cannot fully capture the temporal and sequential characteristics of the PD signal, and they are susceptible to getting stuck in local minima.

The relevant literature explores machine learning methods for gas-insulated switchgear (GIS) failure detection. It highlights the developments in deep learning techniques, demonstrating how they can greatly increase the accuracy of defect diagnostics and improve the dependability and upkeep of GIS technology. Still, several difficulties are mentioned based on the existing fault diagnosis. Traditional models such as BP neural network and SVM are prone to getting stuck in local optima and find it difficult to handle the temporal characteristics of PD signals; Although CNN based methods can extract spatial features, their ability to capture the dynamic evolution of time series is insufficient; Partial hybrid models have high computational complexity and poor real-time performance. Moreover, existing methods heavily rely on a large amount of high-quality annotated data, resulting in significant performance degradation in rare fault samples, and the model's generalization ability needs to be improved. Furthermore, substantial high-quality data must be readily available for these strategies to be effective, which can be challenging in industrial settings. Ensuring these techniques are flexible and scalable is another difficulty because they must be resilient enough to deal with changes in various kinds of GIS equipment and operational environments. These obstacles must be overcome if sophisticated defect detection techniques are to be widely used in the industry. Current research in diagnosing the condition of metal-enclosed gas-insulated devices indicates a few main limitations. Conventional machine-learning models for partial discharge (PD) signals (e.g., BP neural networks and Support Vector Machines) cannot fully capture the temporal and sequential characteristics of the PD signal, and they are susceptible to getting stuck in local minima. Hybrid models which combine Convolutional Neural Networks with recurrent units (e.g., GRU or BiLSTM) can leverage spatial information, but they tend to suffer from high computational overhead and inadequate real-time performance. Additionally, most models involve learning from large amounts of high-quality annotated data, which could greatly reduce model performance, especially in areas where rare fault types are involved, and less generalization performance across fault types. Thus, the accuracy and actual value of the diagnostic models for industrial condition monitoring are limited.

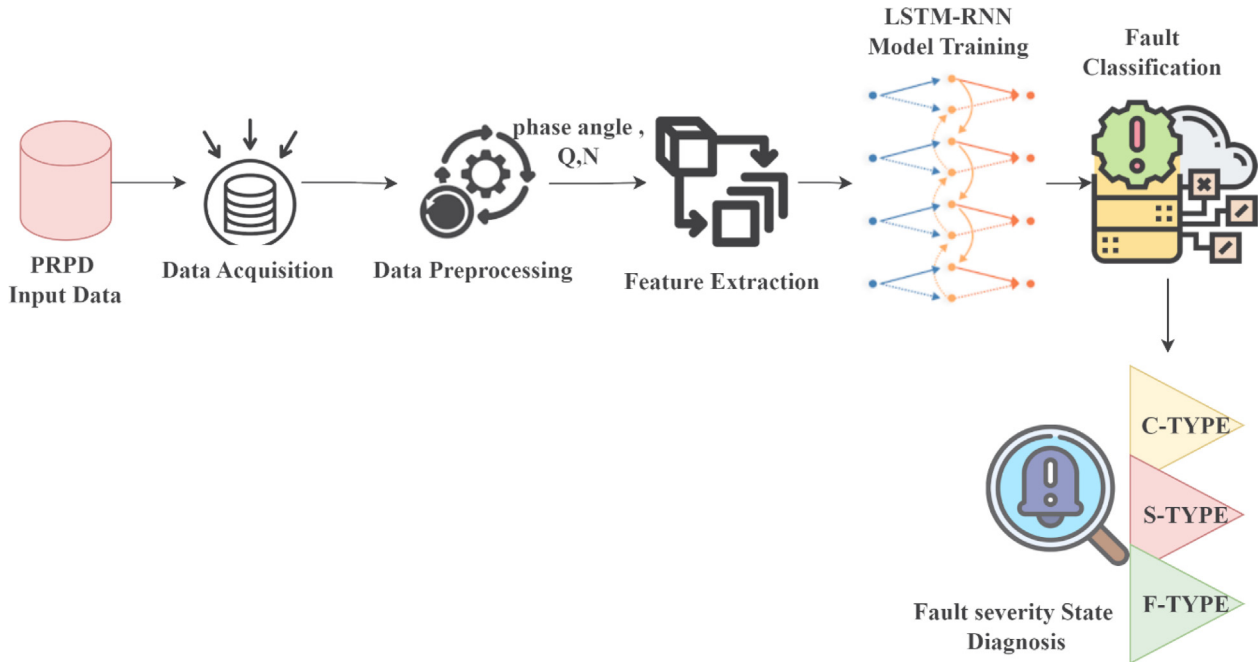


Fig. 1. Graphical representation of LSTM-GISD.

3 Research methodology

3.1 Rationale and architecture overview

The development of the Long Short-Term Memory based diagnosis method network structure is predominantly rooted in the following considerations. Partial Discharge signals are noted to have significant temporal correlations in sequence, coupled to the voltage phase cycle in evolving patterns. The gating mechanism of Long Short-Term Memory network learns long-term relationships in sequences to alleviate the gradient vanishing issue present in standard recurrent neural networks. Unlike models that engage in two-stage spatio-temporal analysis, such as CNN-GRU or CNN-BiLSTM, LSTM structure provides a more direct modeling of temporal dynamic features, thereby enhancing computational efficiency compared to the spatio-temporal analysis process, which is more suited for online diagnostic timeframes. The PD signal is essentially a time-series data strongly correlated with the phase of the AC voltage, and its pattern evolution contains key information about the insulation state of the equipment. The existing methods are difficult to effectively capture the long-term dependencies of this time series. LSTM, with its unique gating mechanism, can selectively remember or forget historical information, making it very suitable for modeling the dynamic temporal characteristics of PD signals. Based on the powerful sequence learning ability of LSTM and combined with multi-source sensor data, an LSTM-GISD model is constructed to accurately identify fault types such as C, S, and F, especially to improve the diagnostic ability for rare F-type faults, thereby achieving more accurate and efficient intelligent diagnosis of GIS equipment status. Data collection, feature extraction, and learning model phase are provided in a

step-by-step analysis in this research, and aims to improve accuracy and performance in real time. For the purpose to strengthen the system more resilient, Improvements in equipment reliability and the efficacy of fault states maintenance procedures for high-voltage power systems are the primary goals of this research. The insulation will deteriorate and eventually fail due to partial discharge, even though it is minor in size. Insulation failure, if unattended, can put diagnosis procedures at risk while also cutting off supplies to customers. Figure 1 illustrates the layout of proposed LSTM-GISD method.

In Figure 1, the LSTM network structure mainly consists of three parts: input layer, hidden layer, and output layer. The input layer receives preprocessed and feature extracted partial discharge signal data, including temporal feature vectors such as main frequency, average discharge amount, and spectral entropy. The hidden layer is the core part, consisting of one or more stacked LSTM units. Each unit selectively remembers or forgets historical state information through the synergistic effect of forget gates, input gates, and output gates, effectively capturing and learning the long-term dependencies and dynamic evolution characteristics of partial discharge patterns in time series. The output layer includes a fully connected dense layer and a Softmax classifier, which maps the final hidden state output by the LSTM layer to the probability distribution of “C-type, S-type, F-type” device states, achieving accurate classification and diagnosis of fault types.

3.2 Dataset composition

The dataset comprises 418 phase-resolved partial discharge patterns generated from a 220 kV GIS experimental platform. Defect models include conductor protrusions, insulator surface contamination, floating electrodes, and

clean reference conditions. Partial discharge signals were acquired using both the ultra-high frequency (UHF) method and the pulse current method to ensure signal diversity and measurement cross-validation. The applied voltage was maintained at 550 kV during defect simulation, with an inception voltage of 385 kV. Gas pressure was stabilized at 0.5 MPa using an SF₆ gas handling system with real-time monitoring. Environmental temperature was controlled at 25 ± 2 °C to minimize thermal drift effects on sensor readings. Data acquisition was repeated three times for each defect type to ensure reproducibility. The F-type samples, though limited to nine instances, were collected under identical conditions to maintain consistency. All raw signals were timestamped and synchronized with the AC voltage phase using a zero-crossing detector. The dataset is publicly available via the cited Mendeley repository, enabling independent validation.

The dataset consists of 418 phase-resolved partial discharge patterns, focusing on different PD types, including a small number of F-types to handle imbalances in the dataset [28]. Coverage of all possible PD types is guaranteed by simulating them in a controlled environment with variable conditions. Gather a varied dataset by simulating C, S, and F partial discharges in a gas-insulated switchgear system. The input voltage sensor detects a 5 Mv spike at a 45° phase angle.

3.3 Data preprocessing

Raw partial discharge data were first subjected to baseline drift removal using a high-pass filter with a cutoff frequency of 10 kHz. Subsequently, noise suppression was performed via wavelet denoising with a Daubechies-4 mother wavelet and soft thresholding. Phase-resolved patterns were constructed by binning discharge events into 72 phase windows of 5° each across the 360° AC cycle. Each discharge event was represented as a triplet (φ , q , n), where φ denotes phase angle in degrees, q is the apparent charge in picocoulombs, and n is the pulse count within the phase bin. Missing bins were interpolated using linear interpolation to ensure uniform sequence length for LSTM input. Normalization was applied per feature dimension using min-max scaling to the range [0,1]. The preprocessed sequences were segmented into fixed-length windows of 100 time steps with 50% overlap to capture both transient and sustained discharge behaviors. Data augmentation was not applied to avoid artificial inflation of rare fault samples. This preprocessing pipeline ensures compatibility with the temporal input requirements of the LSTM architecture while preserving the physical meaning of discharge characteristics.

Data is collected from gas-insulated switch gear equipment with simulated defects with PD patterns, which it is recorded as a function of time and is often represented in terms of phase-resolved partial discharge patterns. The patterns are described in the phase angle of the AC voltage waveform in the form of tuples (\emptyset , Q , N) where \emptyset represents the phase angle of the applied voltage, Q indicates the charge magnitude detected, and N represents the number of discharges.

3.4 Feature extraction

The frequency composition nature of PD signals in gas insulated equipment often varies with time, making them dynamic. Depending on the fault type, severity level, and operating state conditions, the fault diagnostic signals may carry complicated information that varies over a period. With the help of a window function, short time Fourier transform partitions the PD input signal into smaller time intervals. After that, each segment can be shifted into its frequency domain to extract the temporal variation in the frequency content. For capturing the transitory character of PD signals, this specialized analysis is significant. The features are extracted from the PD signals includes statistical measures as

– Dominant frequency

Dominant frequency f_{dom} identifies the frequency at which the highest energy is concentrated in the PD signal where $X(f)$ indicates the magnitude spectrum of the signal, obtained from the fourier transform and this help in distinguishing between these state types using equation (1). This quantity is computed from the magnitude spectrum of phase-resolved partial discharge signals recorded by the Omicron MPD600 system under a 550 kV simulated defect voltage in a 220 kV GIS experimental platform filled with SF₆ at 0.5 MPa.

$$f_{\text{dom}} = \operatorname{argmax}_f |X(f)|. \quad (1)$$

– Mean discharge magnitude

The purpose of mean discharge magnitude \bar{Q} provides an average measure of the discharge magnitude, which helps assess the overall discharge activity level in a piece of gas-insulated equipment using equation (2). The mean discharge magnitude is derived from 418 phase-resolved partial discharge patterns collected using the pulse current method on conductor protrusion, insulator surface contamination, and floating electrode defect models in the laboratory GIS test rig, where apparent charge values were measured in picocoulombs by the Omicron MPD600 instrument.

$$\bar{Q} = \frac{1}{N} \sum_{i=1}^N Q_i \quad (2)$$

Where Q_i indicates the charge magnitude of the i^{th} discharge and N indicates the total number of discharges.

– Standard deviation

The statistics measure standard deviation σ_Q measures the variability or dispersion in discharge magnitudes, helping understand the consistency of discharge events derived from equation (3). The standard deviation of discharge magnitudes is calculated from the same set of 418 PRPD patterns acquired under controlled 550 kV excitation, with charge quantification performed by the Omicron MPD600's calibrated current transducer.

$$\sigma_Q = \sqrt{\frac{1}{N} \sum_{i=1}^N (Q_i - \bar{Q})^2}. \quad (3)$$

Table 1. Phase angle distribution of PD occurrences.

Partial discharge type	Phase angle interval: 0°–90°	Phase angle interval: 90°–180°	Phase angle interval: 180°–270°	Phase angle interval: 270°–360°
Conductor protrusion defect	25%	35%	25%	15%
Insulator surface contamination defect	20%	30%	30%	20%
Floating electrode defect	30%	20%	30%	20%

– Peak discharge magnitude

Peak discharge magnitude Q_{peak} identifies the maximum charge magnitude observed, which is crucial for detecting severe discharge events with an Q array of discharge magnitudes derived using equation (4). The peak discharge magnitude is determined from the maximum apparent charge observed across all discharges in each of the 418 recorded PRPD samples, where charge values originated from the Omicron MPD600's high-resolution digitizer operating at 100 MS/s sampling rate.

$$Q_{\text{peak}} = \max(Q). \quad (4)$$

– Spectral entropy and centroid

The Spectral entropy measures the randomness or complexity of the frequency distribution in which the $P(f)$ indicates the normalized power spectrum and f indicates the frequency. The corona discharges in the sample PD signals have lower entropy than more complex discharges like floating electrode discharges calculated using equations (5) and (6). Spectral entropy is computed from the normalized power spectrum of short-time Fourier transforms applied to 10-millisecond segments of raw partial discharge waveforms, which were captured at 50 MHz sampling rate by the Omicron MPD600 during 550 kV stress tests on the 220 kV GIS defect simulation platform.

$$H_{\text{spec}} = - \sum_f P(f) \log P(f) \quad (5)$$

$$P(f) = \frac{|X(f)|^2}{\sum_f |X(f)|^2}. \quad (6)$$

The extracted features from the PD signals are fed into the Long Short-Term Memory recurrent neural network for classification and fault severity assessment. The spectral centroid C_{spec} provides a measure of the center of mass of the frequency spectrum, indicating that most of the energy is concentrated in metal-enclosed gas-insulated switchgear with $|X(f)|$ indicates the magnitude spectrum. The flow of energy across frequencies can vary across PD types and severity levels; this characteristic helps to understand these differences given in equation (7). The spectral centroid is derived from the magnitude spectrum of the same short-time Fourier transformed PD waveforms used for entropy calculation, all originating from the Omicron MPD600's time-domain recordings

under SF₆ pressure of 0.5 MPa and ambient temperature of 25 °C.

$$C_{\text{spec}} = \frac{\sum_f f \cdot |X(f)|}{\sum_f |X(f)|}. \quad (7)$$

– PD Analysis from the extracted features

The phase angle distribution of PD occurrences across different phases of the AC voltage cycle is crucial for understanding the behavior and features of PD types in high-voltage equipment. Table 1, showing the phase angle distribution of PDs, is used to analyze how different fault states, C-type, S-type, and F-type, proceed across the AC voltage cycle. C type indicates conductor protrusion defects, often due to sharp edges or protrusions on conductors. S-type suggests insulator surface contamination can occur due to manufacturing defects or environmental factors. F-type points to floating metallic particles or detached components within the GIS. The applied the Long Short-Term Memory recurrent neural network model can learn the features associated with each PD type during the training phase by converting these distributions into sequential analysis.

The trained Long Short-Term Memory recurrent neural network model can predict the type of PD based on the new phase angle distribution data given in Table 1. The model can classify the PD type and provide insights into the fault condition of the gas-insulated equipment. The C-type PDs are more prevalent in the 90°–180° phase range, which could indicate characteristics related to conductor defects or protrusions. By effectively classifying PD types, the Long Short-Term Memory recurrent neural network analyses these sequences, allowing for condition monitoring and fault diagnosis of high-voltage gas-insulated equipment according to their phase angle behavior.

3.5 Model training

The Long Short-Term Memory recurrent neural network uses the extracted features from PD signals as inputs to learn temporal dependencies, classify the PD fault state types, and prepare the sequences of PD patterns to train the model with the attributes. The research objective is to train the LSTM network to classify the PD event's fault state type and evaluate its severity using time-series input data of PD variables. Adam optimizer minimizes the loss

function, which can be considered a For gas-insulated equipment diagnosis and maintenance, these attributes allow the Long Short-Term Memory recurrent neural network better to capture the time-frequency fault features of the PD signals, resulting in more precise classification and severity evaluation in terms of low, medium and high. The input sequence at each time step consists of seven features—dominant frequency, mean discharge magnitude, standard deviation, peak discharge magnitude, spectral entropy, spectral centroid, and phase bin index—extracted from the 418 PRPD patterns recorded during defect simulation experiments using the Omicron MPD600.

$$\mathbf{X}_t = (\emptyset_t, \mathbf{Q}_t, \mathbf{N}_t) \quad (8)$$

Where \mathbf{X}_t in equation (8) indicates the input sequence at time t . The insulator surface of metal-enclosed gas-insulated switchgear can initiate partial discharges (PDs) at various particle terminals with variable spatial information, and the PD modes can vary with respect to the spatial location and the applied voltage phase. The on-site dielectric test's efficacy in defect diagnosis and the mechanism of the PD mode transition are analyzed. The equipment is a metal enclosure, gives a protective barrier to physical states and diagnoses faults. Inside this metal, the equipment is insulated with a gas, typically sulfur hexafluoride gas SF₆, that contains insulating properties to prevent electrical discharges.

The preprocessed input sequence consists of features extracted from PD signals like dominant frequency and spectral centroid, which are fed into the LSTM layers to diagnose the state of the gas-insulated equipment. At each time step t , the LSTM processes the current feature vector with the input vector \mathbf{x}_t , β as the bias term, W indicates the weight update factor and updates the hidden layer state termed as \mathbf{h}_t . The model training of Long Short-Term Memory recurrent neural network is defined using the below equations (9)–(12). The forget gate activation is denoted as f_t , controls the information from the previous cell state \mathbf{c}_{t-1} should be carried forward and help to retrain features irrelevant to the current time step. The analysis ensures that only relevant historical data is considered for diagnosis. The forget gate, input gate, candidate cell state, and output gate activations are computed based on input feature vectors derived exclusively from the Omicron MPD600—recorded phase-resolved partial discharge data under 550 kV applied voltage, 0.5 MPa SF₆ pressure, and controlled laboratory temperature.

$$f_t = \sigma\left(W_f \cdot (\mathbf{h}_{t-1}, \mathbf{x}_t) + \beta_f\right) \quad (9)$$

$$i_t = \sigma\left(W_{ci} \cdot (\mathbf{h}_{t-1}, \mathbf{x}_t) + \beta_i\right) \quad (10)$$

$$\tilde{\mathbf{c}}_t = \tanh\left(W_c \cdot (\mathbf{h}_{t-1}, \mathbf{x}_t) + \beta_c\right) \quad (11)$$

$$\mathbf{c}_t = f_t * \mathbf{c}_{t-1} + i_t * \tilde{\mathbf{c}}_t \quad (12)$$

The LSTM network input unit is defined as \mathbf{x}_t , input gate activation vector is i_t determines how much current PD feature information in the analysis should be integrated into the cell state. This is significant for updating the model with the new PD features that contribute to the current state diagnosis of equipment. The candidate cell state vector $\tilde{\mathbf{c}}_t$ represents potential new states based on current PD data added to the cell state derived from PD features and is non-linearly transformed to ensure the cell state remains within the range of -1 to $+1$.

$$\mathbf{O}_t = \sigma\left(W_o \cdot (\mathbf{h}_{t-1}, \mathbf{x}_t) + \beta_o\right) \quad (13)$$

$$\mathbf{h}_t = \mathbf{O}_t * \tanh(\mathbf{c}_t) \quad (14)$$

The output gate \mathbf{O}_t in equation (13) controls the flow of information from the cell state to the hidden state, decides which part of the cell state should be output as the hidden unit state vector is \mathbf{h}_t in equation (14) is used to make the final diagnosis. The cell input activation vector is $\tilde{\mathbf{c}}_t$, the cell state vector \mathbf{c}_t serves as the memory of the LSTM, holding relevant information for long-term state diagnosis. The hidden state \mathbf{h}_t is the output of the LSTM unit at each time step and serves as the input to subsequent layers or the decoder for classifying the type of PD event or assessing the fault severity. The output of the LSTM contributes to the final diagnosis of the equipment's condition. The computed \mathbf{h}_t vector is given as input to the decoder to identify the faulty state of the gas-insulated equipment with the phase angle difference. The decoder has two layers, such as LSTM layer output, fed into the dense layer to classify the equipment conditions.

3.6 Fault classification

The Long Short-Term Memory recurrent neural network outputs a probability distribution over the possible states derived using equation (15) in terms of $P(\text{state}|\mathbf{X})$ Using a softmax output layer in terms of (normal, C-type, S-type, F-type). The fault types labelled as 1, 2 and 3 for C, S, and F fault types. The softmax output probabilities are computed from the final hidden state of the LSTM, which was trained on 418 labeled samples of partial discharge patterns corresponding to conductor protrusion, insulator surface contamination, and floating electrode defects, all acquired using the Omicron MPD600 in a 220 kV GIS test setup.

$$P(\text{state}|\mathbf{X}) = \text{softmax}(W_s \cdot \mathbf{h}_T + \beta_s) \quad (15)$$

equation (15) provides probabilities for each possible state based on the final hidden state \mathbf{h}_T of the LSTM in which W_s and β_s represents the weight matrix and bias vector for the softmax layer. The decoder part of the LSTM update is given using equation (16).

$$\mathbf{h}'_t = \text{LSTM}(\mathbf{h}'_{t-1}, \mathbf{x}'_t; \theta) \quad (16)$$

The parameter \mathbf{h}_t indicates the decoder's hidden state at time step t , and the \mathbf{x}'_t is the input to the decoder, which could be the hidden state from the previous LSTM layer

Table 2. Fault severity classification.

Partial discharge state types	Low severity	Medium severity	High severity
C-type	$Q < 10 \text{ pC}$	$10 \text{ pC} \leq Q < 50 \text{ pC}$	$Q \geq 50 \text{ pC}$
S-type	$Q < 5 \text{ pC}$	$5 \text{ pC} \leq Q < 30 \text{ pC}$	$Q \geq 30 \text{ pC}$
F-type	$Q < 20 \text{ pC}$	$20 \text{ pC} \leq Q < 80 \text{ pC}$	$Q \geq 80 \text{ pC}$

with a processed version of the features. The final hidden state h_T LSTM is passed through a dense layer with a softmax activation function from the decoder to classify the equipment's normal state. The output is a probability distribution over the possible states: normal, C-type, S-type, and F-type states.

$$\text{pre}_{\text{state}} = \text{argmax}\left(\text{P}(\text{state} | \text{X})\right). \quad (17)$$

The above equation (17) condition states with the highest probability of the final classification. By accurately classifying these fault types, the model provides crucial information for the maintenance and operation of GIS equipment. For instance, the high probability of C-type fault states suggests a need for inspection and possible refinishing of conductor surfaces. The prevalence of S-type faults could indicate a need for cleaning procedures or improved sealing against contaminants. Likewise, the diagnosis of F-type faults needs immediate focus due to the risk of breakdown they indicate.

The inequalities in Table 2 define thresholds that classify the severity of fault states by measuring the charge magnitude during a PD event. PDs produce small amounts of charge, typically measured in the picoCoulomb (pC) range unit in high-voltage equipment like gas-filled in insulated switchgear equipment. The proposed system can determine whether the fault is in low, medium, or high severity states and trigger appropriate responses. From this analysis, operators can prioritize maintenance efforts, especially for high-severity discharges across all PD types, which are critical and need immediate focus to prevent equipment failure and ensure the safety and reliability of the grid lines. Medium severity state needs closer monitoring and possibly proactive maintenance, while low-severity discharges should be tracked over time to diagnose potential failures.

3.7 Fault severity state diagnosis

Depending on the type and level of the equipment state, the system determines the overall health of the equipment. The state of normal condition indicates no significant issues. All equipment in PD patterns is functioning as expected. A severity level such as early warning, rapid deterioration, or critical breakdown is associated with an identified fault type (C, S, or F) to indicate the state of the equipment. Operators can determine if service, repair, or substitute for the equipment is required based on the diagnostics' result. The impact of PD instances can be classified according to their magnitude by considering these state factors. Diagnostic systems evaluate the condition of metal-

enclosed gas-insulated equipment using these thresholds in operation. The system can identify and classify defects into low, medium, or high levels of severity using these criteria, allowing for prompt maintenance activities and guaranteeing the equipment's reliability and safety.

The proposed method approach can process sequential PRPD data, thus capturing the evolution of PD patterns observed in metal-enclosed gas equipment over time. In the LSTM formulations, which mathematically depict this temporal analysis, the output at each time step depends on the input state at that moment and the states that happened before it. This method offers a thorough approach to state diagnosis of metal-enclosed gas insulating complete equipment by coupling dataset attributes to the Long Short-Term Memory recurrent neural network model and the physical form of GIS faults. This could improve maintenance plans and reduce the risk of equipment failure. The observed PRPD patterns showed that discharges were monitored across a voltage range of varying conditions.

4 Performance validation

4.1 Experimental setup and validation protocol

The performance of the Long Short-Term Memory based diagnosis method was validated using the simulation parameters in this table. Different numbers of C-type, S-type, and F-type cases were recorded in the simulations, which used a defect setup rated at 550 kV and included a range of PD patterns. The Omicron MPD600 apparatus was used to take the measurements, with an inception voltage of 385 kV and a pressure of 0.5 MPa. Table 3 discusses the parameters that provide the basis of the performance metrics that measure how well the diagnostic approach works.

4.2 Comparative study analysis

In this section, the study underscores the proposed deep-learning technique's performance ability to enhance fault detection in GIS by comparing it with baseline methods like the back-propagation neural network with support vector machine [17], the convolutional neural network with gated recurrent unit [20], the convolutional neural network with bidirectional long short-term memory [23], and the back-propagation neural network using ultra-high frequency signals [25], although the challenges regarding data requirements and computational efficiency are used for comparison.

Preliminary analysis of benchmarking schemes: BPNN-SVM [17] – A support vector machine (SVM) based on the residual BP neural network is introduced to facilitate the identification of transformer defects.

Table 3. Simulation settings.

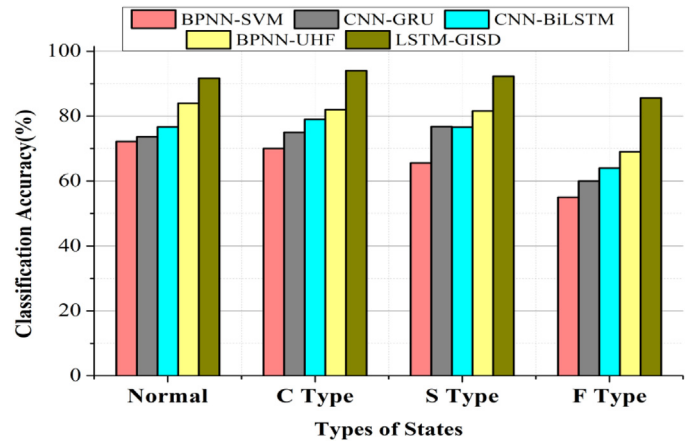
Parameter	Value
Simulated defect set, kV	550
Total PD patterns	C type-280, S type-129, F type-9
Measurement instrument	Omicron MPD600
Inception voltage, kV	385
Gas pressure, MPa	0.5
Performance Metrics	Classification Accuracy, Precision, Recall, F1-score and Computational Time

CNN-GRU [20] – GIS operating state prediction method based on the combined neural network of convolutional neural network (CNN) and gated recurrent unit (GRU). CNN-BiLSTM [23] – To improve the system's capacity to detect partial discharge defects, spatial and temporal correlations are obtained through the use of Convolutional Neural Networks (CNN) and Bidirectional Long-Short-Term Memory (BiLSTM). BPNN-UHF [25] – The proposed diagnostic approach of the BP neural network integrates partial discharge signals from flaws through pulse current and UHF techniques, strengthening the DS evidence theory application.

4.3 Results and discussion

4.2.1 Classification accuracy

Several baseline approaches, such as BPNN-SVM [17], CNN-GRU [20], CNN-BiLSTM [23], and BPNN-UHF [25], are compared to the proposed LSTM-GISD's classification accuracy in Figure 2. The x-axis shows the various fault diagnosed states, and the y-axis shows the percentage of accuracy in classification. In terms of accurately recognizing various fault states of the gas-insulated equipment, as usual, C-type, S-type, and F-type. The proposed LSTM-GISD performs better than the baseline approaches. It demonstrates exceptionally high accuracy regarding the comparatively rare F-type fault states from equations (16) and (18) are used from the LSTM model to analyze the classification model and applied to the test dataset, yielding this result. Compared to traditional methods like PD pattern analysis and gas chromatography, which rely on manual experience or single features, the LSTM-GISD model is more complex but offers significantly improved accuracy. Traditional methods, while less complex, struggle to capture the temporal dynamics of PD signals and the correlation of multi-source information, resulting in low recognition rates for complex defects (such as F-type defects). Although a deep learning model with high computational complexity, LSTM-GISD automatically learns the long-term temporal dependencies of PD patterns and fuses multi-sensor data, effectively overcoming noise interference and sample imbalance.

**Fig. 2.** Classification accuracy analysis.

4.2.2 Precision

Figure 3a shows how accurate LSTM-GISD is in calculating precision and analysis compared to the baseline approaches. The percentage of correct fault state types predicted analysis relative to the total number of optimistic predictions of faults in the complete equipment is known as precision. Values for precision are displayed on the y-axis, with the iteration ranges from 10 to 100 counts listed on the x-axis. The recall with Figure 3b for LSTM-GISD in comparison to the baseline approaches is displayed in this graph. The recall metric quantifies the accuracy with which different types of errors were diagnosed.

4.2.3 F1-Score

Figure 4 illustrates the comparison between the F1-Score of LSTM-GISD and the baseline methods. The F1-Score is a metric that combines precision and recall, creating a balance between the two analysis. The methods are analyzed with the iteration count on the x-axis, and the F1-Score values are shown on the y-axis. The F1-Score ensures that the system for diagnosis can reliably distinguish between different types of fault states with low error rates and high accuracy, which enhances taking decisions for repair and operational strategies by Long Short-Term Memory recurrent neural network model training. The LSTM-GISD model maintained high scores at different iterations and was significantly better than baseline models such as the back-propagation neural network combined with support vector machine and the convolutional neural network combined with gated recurrent unit. This indicates that the model not only combines the advantages of accuracy and recall, but is also effective in identifying rare fault categories. Moreover, its performance is stable throughout the entire training process and is not easily affected by iterative fluctuations. This result verifies that LSTM-GISD has stronger robustness and generalization ability in handling imbalanced GIS fault data, providing support for achieving reliable state diagnosis. The LSTM-GISD model maintains high

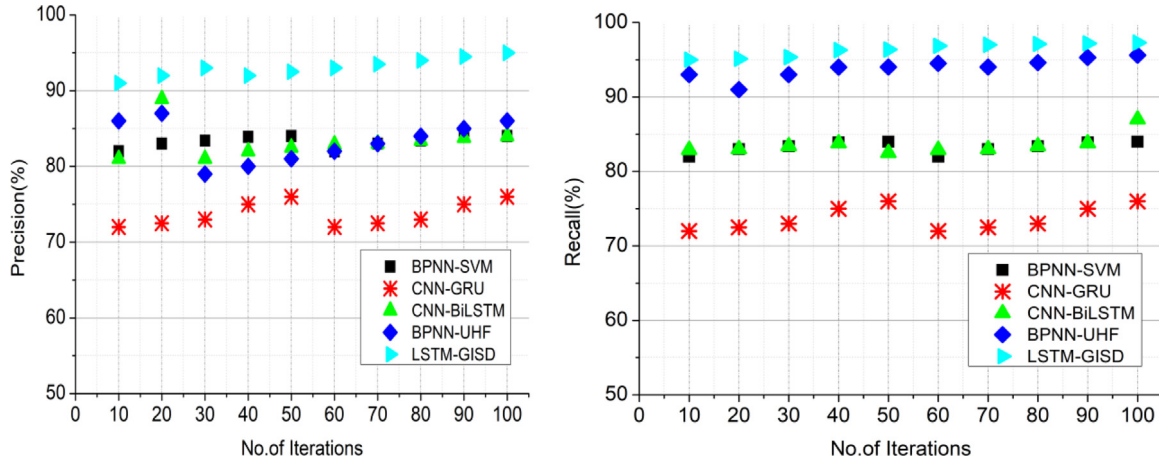


Fig. 3. State diagnosis efficiency in terms of (a) Precision analysis, (b) Recall analysis.

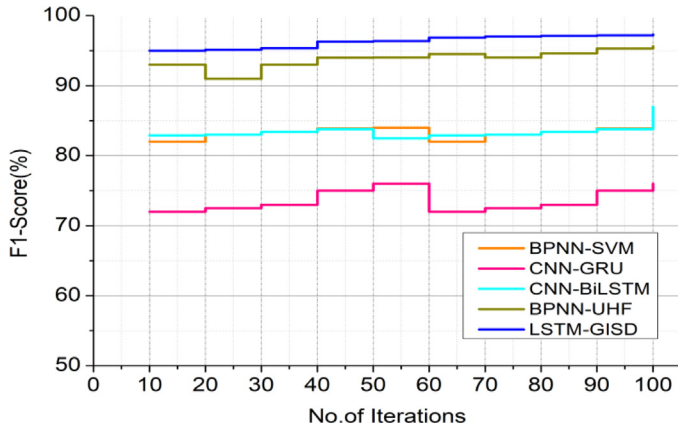


Fig. 4. F1-score analysis on varying iterations.

F1-scores across varying iterations and significantly outperforms baseline models, indicating a good balance between precision and recall. This result demonstrates that the model possesses stronger robustness and generalization capability when handling imbalanced GIS fault data. It effectively identifies rare fault categories and delivers stable performance throughout the training process, unaffected by iterative fluctuations, which provides reliable support for fault diagnosis and maintenance decision-making in practical applications.

4.2.4 Computational time

As each technique is executed for identifying the faults, the computational time is measured empirically using Figure 5. The model keeping track of insulated components like how long it takes for each technique to process the data samples like conductors and floating rods. The graphic below shows a comparison of the computing time needed by LSTM-GISD and different baseline approaches. The methods are listed on the x-axis, and the time taken is shown on the y-axis in seconds. Figure 1 shows that LSTM-GISD outperforms competing methods in terms of efficiency, even though it has a complex architecture. For ensuring the dependability of gas-insulated switchgear (GIS) systems, real-time applications want faster computational time for

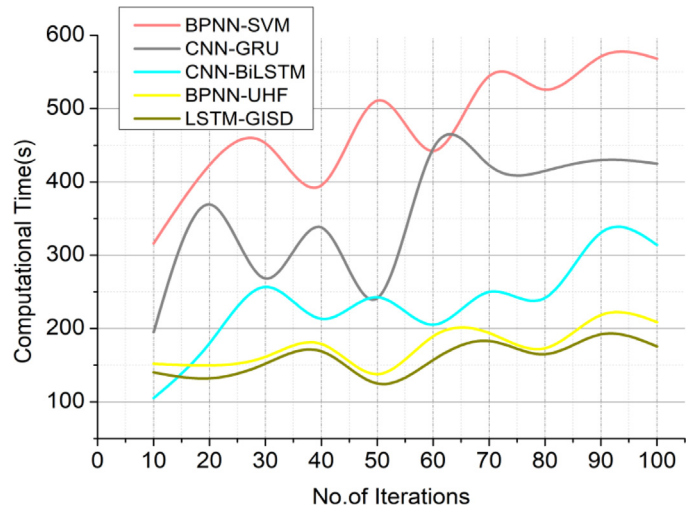


Fig. 5. Calculation of computational time.

rapid fault state diagnosis. LSTM-GISD improves computational efficiency while maintaining high accuracy by optimizing network structure and utilizing GPU acceleration. Its computation time is superior to various baseline methods, and it has strong real-time diagnostic potential. This method can quickly identify C, S, and F types of faults, especially with high robustness for rare F-type defects. It can achieve online monitoring and early warning of GIS equipment, providing efficient and reliable state diagnosis support for high-voltage power grids, and has important application value.

5 Conclusion

The study successfully achieves its aim of developing an accurate, real-time capable state diagnosis method for metal-enclosed gas-insulated equipment through a Long Short-Term Memory based framework that effectively captures temporal dynamics of partial discharge signals and improves recognition of rare fault types. The method works based on Long Short-Term Memory with the accurate diagnosis and classifies the PD patterns linked

to different fault types, including the difficult F-type faults, by utilizing DL algorithms. With the consideration of variations in time in PD signals, the LSTM-GISD method outperforms conventional methods in terms of comes to classified PD data. The system's real-time monitoring capabilities also allow for preventative maintenance, which could lessen failures of gas insulated equipment. By including environmental component analysis, the model's predictive skills are further enhanced, guaranteeing reliability in a variety of operational settings. This research proposes an LSTM-GISD method for state diagnosis of metal-enclosed gas-insulated equipment. The results demonstrate that the proposed method achieves superior performance in classification accuracy, precision, recall, and F1-score compared to baseline models, exhibiting particularly strong recognition capability for rare and critical F-type faults. The LSTM-based architecture effectively captures the temporal dynamics of partial discharge signals, enhancing diagnostic accuracy and robustness. Furthermore, the model demonstrates high computational efficiency and holds potential for real-time diagnosis, providing reliable technical support for the intelligent and precise predictive maintenance of high-voltage equipment. The experiment shows that the model outperforms various baseline methods in classification accuracy, precision, recall, and F1 score, especially exhibiting strong recognition ability for rare and dangerous F-type faults. Its architecture based on LSTM can effectively capture the temporal dynamic characteristics of partial discharge signals, improving the accuracy and robustness of diagnosis. At the same time, the model has high computational efficiency and the potential for real-time diagnosis, providing reliable technical support for the intelligent, precise and predictive maintenance of high-voltage equipment, and has important engineering application value. As a whole, the study makes an important contribution in high-voltage electric grid networks with metal enclosed gas insulated equipment by providing an improved method to diagnose gas-insulated equipment's health; this opens the door to safer and more reliable equipment. However, there are still limitations to this article. The model training in this article relies on defect data simulated in the laboratory, which may differ from the complex noise and variable operating conditions in the actual operating environment, affecting the generalization ability of the model. The model mainly focuses on three typical types of defects: C, S, and F. Its ability to identify other types of defects or new faults needs further verification. Future work will focus on applying transfer learning algorithms for diagnosing the equipment status in each operational state for improving the diagnosis accuracy and more fault state analysis and thereby reduced the gas insulated equipment failures. By integrating more sensor data and building multimodal inputs, the comprehensiveness and robustness of diagnosis can be improved. Furthermore, more advanced deep learning architectures, such as Transformer or spatiotemporal graph neural networks, can be explored to better capture the long-range dependencies and spatial correlations of PD signals, thereby realizing an adaptive, highly accurate intelligent diagnostic system.

Glossary

Gas-Insulated Switchgear (GIS)	A compact power distribution unit enclosing high-voltage components in a metal casing filled with SF6 gas.
Partial Discharge (PD)	Non-penetrating discharges occurring in localized areas of dielectrics.
Phase-Resolved Partial Discharge (PRPD)	Analysis method for correlating the discharge volume and frequency of partial discharges with the voltage phase at which they occur.
Long Short-Term Memory (LSTM)	A recurrent neural network that effectively captures long-term dependencies in time series.
Recurrent Neural Network (RNN)	A variant of the LSTM, a type of neural network with internal recurrent connections that excels at processing sequential data.
Back-Propagation Neural Network (BPNN)	A multi-layer feedforward neural network trained using the back-propagation error algorithm.
Convolutional Neural Network (CNN)	A deep neural network that automatically extracts spatial features from input data through convolution operations.
Gated Recurrent Unit (GRU)	A simplified version of the LSTM, controlling information flow through update and reset gates.
Bidirectional LSTM (BiLSTM)	A network consisting of forward and backward LSTMs.
Support Vector Machine (SVM)	A supervised learning algorithm that maximizes the classification margin by finding an optimal hyperplane.
Ultra-High Frequency (UHF)	A detection technology for locating and evaluating discharges by detecting 300 MHz-3 GHz electromagnetic wave signals generated by PDs.

Funding

This work is supported by Science and Technology Project of State Grid Sichuan Electric Power Company (Project No. 52199723001C).

Conflicts of interest

The authors have nothing to disclose.

Data availability statement

This article has no associated data generated.

Author contribution statement

Conceptualization: J. W.; Methodology: J. W. and D. Z.; Software: J. W., D. Z. and Y. F.; Validation: X. L. and Y. Z.; Formal analysis: Y. H.; Investigation: Z. L., Y. H. and X. L.; Writing - Original Draft: J. W., D. Z. and Y. F.; Writing - Review & Editing: Z. L., Y. H., X. L. and Y. Z.; Supervision: Y. Z.

References

- [1] Y. Wang, J. Yan, Z. Yang, Z. Qi, J. Wang, Y. Geng, A novel hybrid meta-learning for few-shot gas-insulated switchgear insulation defect diagnosis, *Expert Syst. Appl.* **233**, 120956 (2023)
- [2] G.V. Xavier, H. S. Silva, E.G. Da Costa, A.J. Serres, N.B. Carvalho, A.S. Oliveira, Detection, classification and location of sources of partial discharges using the radiometric method: trends, challenges and open issues, *IEEE Access* **9**, 110787–110810 (2021)
- [3] T. Shahsavarian, Y. Pan, Z. Zhang, C. Pan, H. Naderiallaf, J. Guo, Y. Cao, A review of knowledge-based defect identification via PRPD patterns in high voltage apparatus, *IEEE Access* **9**, 77705–77728 (2021)
- [4] Z. Faizol, F. Zubir, N.M. Saman, M.H. Ahmad, M.K.A. Rahim, O. Ayop, Z. Yusoff, Detection method of partial discharge on transformer and gas-insulated switchgear: a review, *Appl. Sci.* **13**, 9605 (2023)
- [5] N. Rosle, N.A. Muhamad, M.N.K.H. Rohani, M.K.M. Jamil, Partial discharges classification methods in XLPE cable: a review, *IEEE Access* **9**, 133258–133273 (2021)
- [6] N.A. Muhamad, I.V. Musa, Z.A. Malek, A.S. Mahdi, Classification of partial discharge fault sources on SF₆ insulated switchgear based on twelve by-product gases random forest pattern recognition, *IEEE Access* **8**, 212659–212674 (2020)
- [7] A.S. Mahdi, Z. Abdul-Malek, R.N. Arshad, SF₆ decomposed component analysis for partial discharge diagnosis in GIS: A review, *IEEE Access* **10**, 27270–27288 (2022)
- [8] Z. Wu, B. Lyu, Q. Zhang, L. Liu, J. Zhao, Phase-space joint resolved PD characteristics of defects on insulator surface in GIS, *IEEE Trans. Dielectr. Electr. Insul.* **27**, 156–163 (2020)
- [9] F. Zeng, B. Xie, D. Su, C. Li, Z. Lei, G. Ma, J. Tang, Breakdown characteristics of eco-friendly gas C₅F₁₀O/CO₂ under switching impulse in nonuniform electric field, *IEEE Trans. Dielectr. Electr. Insul.* **29**, 866–873 (2022)
- [10] H. Li, K. Zhao, J. Yang, S. Gao, Contact defect detection of gas insulated line via thermal-vibration feature fusion and deep neural network technique, *IEEE Trans. Instrum. Meas.* (2023)
- [11] D. Nguyen, Analytical Modeling and Simulation of Capacitive Micromachined Ultrasonic Transducer, 2020
- [12] H.K. Sandhu, S.S. Bodda, A. Gupta, A future with machine learning: review of condition assessment of structures and mechanical systems in nuclear facilities, *Energies* **16**, 2628 (2023)
- [13] S. Mantach, Supervised and Unsupervised Deep Learning Models for Partial Discharge Source Detection and Classification in Electrical Insulation, 2023
- [14] L. Duan, J. Hu, G. Zhao, K. Chen, J. He, S.X. Wang, Identification of partial discharge defects based on deep learning method, *IEEE Trans. Power Deliv.* **34**, 1557–1568 (2019)
- [15] Z. Wu, Q. Zhang, J. Ma, X. Li, T. Wen, Effectiveness of on-site dielectric test of GIS equipment, *IEEE Trans. Dielectr. Electr. Insul.* **25**, 1454–1460 (2018)
- [16] A. H. Alshalawi, F. S. Al-Ismail, Partial discharge detection based on ultrasound using optimized deep learning approach, *IEEE Access* (2024)
- [17] Y. Jin, H. Wu, J. Zheng, J. Zhang, Z. Liu, Power transformer fault diagnosis based on improved BP neural network, *Electronics* **12**, 3526 (2023)
- [18] V.N. Tuyet-Doan, Y.W. Youn, H. S. Choi, Y.H. Kim, Shared knowledge-based contrastive federated learning for partial discharge diagnosis in gas-insulated switchgear, *IEEE Access* (2024)
- [19] A.S. Karandaev, I.M. Yachikov, A.A. Radionov, I.V. Liubimov, N.N. Druzhinin, E. A. Khramshina, Fuzzy algorithms for diagnosis of furnace transformer insulation condition, *Energies* **15**, 3519 (2022)
- [20] J. Li, A. Zhang, W. Yang, Research on state prediction of gas insulated switchgear based on CNN-GRU combinatorial neural network, in: 2022 IEEE 6th Conference on Energy Internet and Energy System Integration (EI2), 2022, pp. 2294–2298
- [21] Y.A.M. Alsumaidae, C.T. Yaw, S.P. Koh, S. K. Tiong, C.P. Chen, T. Yusaf, A.A. Raj, Detection of corona faults in switchgear by using 1D-CNN, LSTM, and 1D-CNN-LSTM methods, *Sensors* **23**, (2023)
- [22] X. Bampoula, N. Nikolakis, K. Alexopoulos, Condition monitoring and predictive maintenance of assets in manufacturing using LSTM-autoencoders and transformer encoders, *Sensors* **24**, 3215 (2024)
- [23] W. Hu, J. Li, X. Liu, G. Li, Partial discharge fault identification method for GIS equipment based on improved deep learning, *J. Eng.* **2024**, e12386 (2024).
- [24] W. Sun, H. Ma, S. Wang, (2024). A Novel Fault Diagnosis of GIS Partial Discharge Based on Improved Whale Optimization Algorithm, *IEEE Access.* (2024)
- [25] Y. Cong, K. Tang, Z. Li, Z. Liu, B. Chen, Y. Liu, Y. Fang, GIS equipment fault identification based on BP neural network and improved DS evidence fusion, *J. Electr. Eng.* **18**, 361–369 (2024)
- [26] A. Pulikkathodi, E. Lacazedieu, L. Chamoin et al., A neural network-based data-driven local modeling of spotwelded plates under impact, *Mech. Ind.* **24**, 34 (2023)
- [27] T. Xia, L. Zhou, L. Quan, The study on surface defect detection of stamped parts based on improved deep learning, *Mech. Ind.* **26**, 27 (2025)
- [28] <https://data.mendeley.com/datasets/cz8gwg9d2v/1>

Cite this article as: J. Wang, D. Zhou, Y. Fang, Z. Long, Y. He, X. Luo, Y. Zou, The state diagnosis method of metal enclosed gas insulation complete equipment based on deep learning algorithms, *Mechanics & Industry* **27**, 5 (2026), <https://doi.org/10.1051/meca/2026001>